Aust. J. Phys., 1977, **30**, 591–7

Gamma Rays from keV Neutron Capture in Lanthanum

M. J. Kenny and B. J. Allen

AAEC Research Establishment, Private Mail Bag, Sutherland, N.S.W. 2232.

Abstract

A Ge(Li) detector has been used to observe γ-ray transitions after the capture of keV neutrons in lanthanum. An analysis of nonstatistical transitions to low-lying $l_n = 3$ final states supports the proposed particle–hole capture mechanism.

Introduction

The neutron capture mechanism for γ-ray transitions to final states with large angular momenta has been investigated recently for scandium and lanthanum (Allen *et al.* 1976). It was found that neither the statistical nor valence models could account for the anomalous γ-ray intensities which were observed and a two-particle, one-hole mechanism was invoked to explain the data. While measurements with both Ge(Li) and NaI detectors had been made previously for a range of neutron energies in scandium, only one NaI measurement at 210 keV was available for lanthanum. Indirect evidence discounted the role of d-wave capture in this measurement, but direct measurement of the d-wave component would have been preferred. One method of achieving this is to observe the intensity of transitions to the 0^- and 7^- states in lanthanum at excitations of 581·1 and 284·6 keV respectively, since electric dipole transitions to these states can only occur after $d_{5/2}$ neutron capture. The proposed explanation was therefore tested here by observing capture spectra with a Ge(Li) detector for the neutron energy range 10–70 keV.

Experiment

The well-established technique in this laboratory (Kenny *et al.* 1976) is to use a pulsed and bunched proton beam from the 3 MeV Van de Graaff accelerator to irradiate a lithium target at an energy several keV above the neutron threshold. This produces a forward cone of neutrons with energies between 10 and 70 keV. The capture sample is located in the cone some 25 cm from the neutron source. A shielded Ge(Li) detector measures both γ-ray energy and neutron flight time and spectra are recorded for digital windows corresponding to different neutron flight times. In the present experiment a CAMAC-controlled digital to analogue stabilization was used to maintain an energy stability of $\pm 0 \cdot 5$ keV. Reference peaks used were the 2614 keV line from a ^{228}Th source and the equivalent of 6000 keV from a research pulser.

The capture sample contained 1·0 kg of La_2O_3 in powder form, held in a magnesium holder (80 g) of 15·0 cm diameter and 3·0 cm thick. The running time was 112 hr for an average beam current of 7 μA.

Gamma ray spectra were obtained for three neutron energy regions and one background region. The spectra covered the range 2590–6050 keV at 1·67 keV per channel. Since the binding energy of $^{139}La(n,\gamma)$ is 5161 ± 1 keV (Jurney *et al.* 1970), calibration lines close to this energy were chosen. Thermal capture by silicon provides strong lines at $3595\cdot2 \pm 0\cdot5$ and $4934\cdot3 \pm 0\cdot4$ keV (Spits *et al.* 1971). The neutron beam was thermalized and a 1 kg sample of natural silicon was used to obtain a calibration spectrum.

The Ge(Li) detector efficiency relative to NaI at 1333 keV was 21%. In the energy region of most importance in this experiment (4–5 MeV), the ratio of full energy, single and double escape peaks is 2·0 : 1·6 : 1·0.

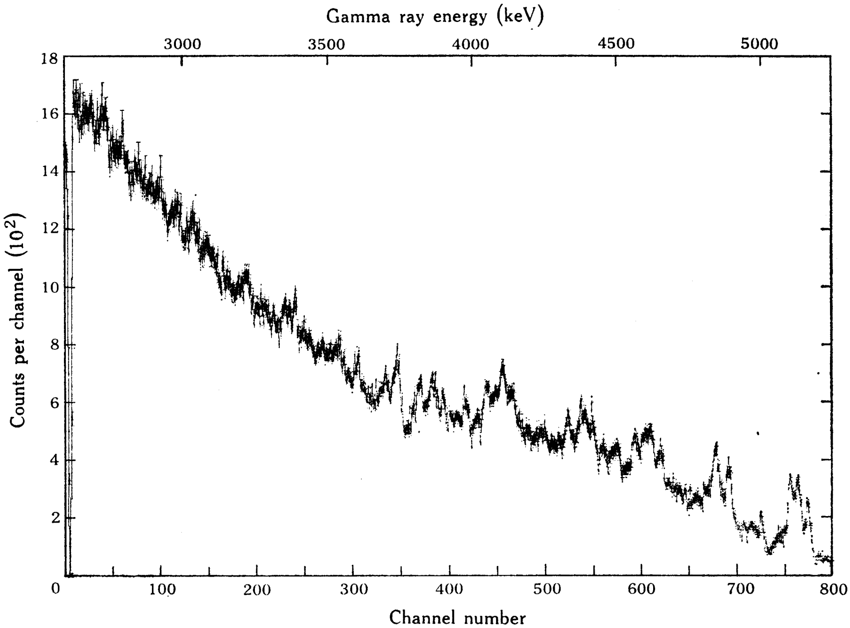

Fig. 1. Average capture γ-ray spectrum from ^{139}La for neutron energies in the range 10–70 keV.

Results

Since the average resonance spacing in ^{139}La is 150 eV (Mughabghab and Garber 1973), the spectra obtained in each digital window were averaged over 50–100 resonances. In addition, there was some smearing between windows due to the beam pulse width and the relatively thick lanthanum sample.

The capture γ-ray spectra were shifted by 30, 42 and 53 keV respectively, to correct for the shift in the primary γ-ray energy due to the different incident neutron energy in the three regions considered. The spectra were then summed and the background was subtracted. This produced a spectrum averaged over the neutron energy range 10–70 keV. Some broadening of the γ-ray peaks necessarily remained.

The resultant average γ-ray spectrum is shown in Fig. 1. Very few resolved peaks are observed below 3·6 MeV and the lower portion of the spectrum has some resemblance to a statistical shape. At higher energies, the spectrum shows numerous resolved peaks. The high energy portion of the spectrum is given in Fig. 2 after

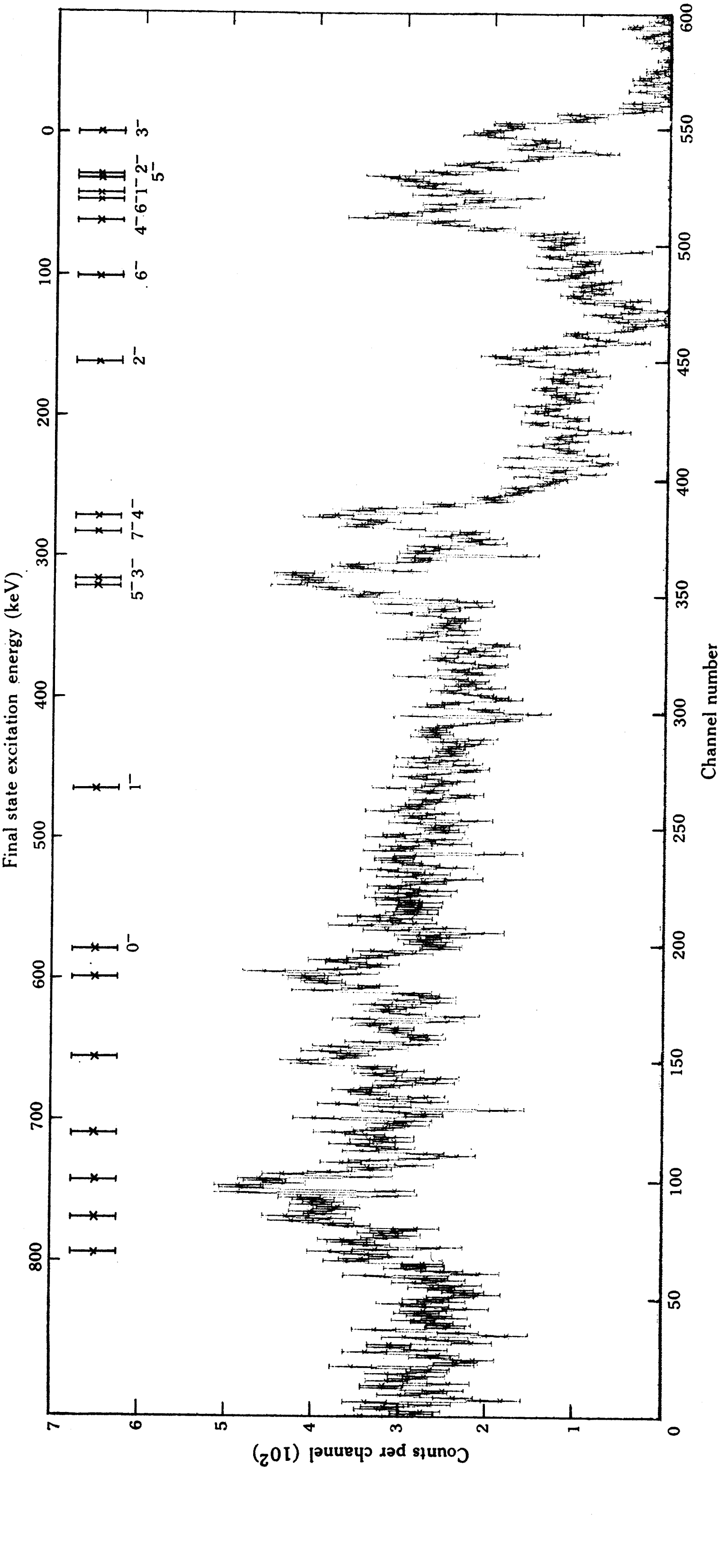

Fig. 2. Primary γ-ray spectrum obtained from the high energy portion of Fig. 1 after subtraction of single escape peaks. The energies and known spins and parities of the first 20 levels in ^{140}La are indicated.

correction for single escape peaks. Care was taken to ensure an accurate correction as a single escape peak of the 5098 keV γ-ray falls close to the expected position of the 4580 keV γ-ray to the 0^- state. The positions of the first 20 levels in ^{140}La are shown in Fig. 2 using the level scheme of Jurney *et al.* (1970). Individual γ-ray intensities fluctuate with neutron energy, but the statistics are inadequate to obtain a reliable neutron energy dependence.

Table 1. Observed intensities in neutron capture by ^{139}La

(1) E_γ (keV)	(2) E_x[A] (keV)	(3) l_n[B]	(4) J_f^{π}[A]	(5) Present 10–70 keV relative intensity[C]	(6) Thermal intensity[A]	(7) (d, p) intensity[B]
5161±2	0	3	3^-	8±1	3·4	13·6
5131±2	30·0	3	2^-	14±3 (rows 5131–5112): 7±3	4·8 (rows 5131–5126)	14·4
5126±2	34·7	3 (rows 5126–5117)	5^-	4±2		21·2
5117±2	43·8		1^-	1·5±1·0		—
5112±2	48·9	3	6^-	1·5±1·0		30·4
5098±2	63·2	3	4^-	12±2	25·8	20·5
5057±2	103·8		6^-	1·0±0·5		—
4998±2	162·7	3	2^-	2·5±0·5	0·6	6·0
4889±2	272·3		4^-	16±3 (rows 4889–4876): 15±3		—
4876±2	284·6	3	7^-	1^{+2}_{-1}		35·7
4843±2	318·2	(3)	3^-	22±4 (rows 4843–4839): 12±4	27·2	3·3
4839±2	322·0		5^-	10±4		—
4693±2	467·5	3	1^-	<1		2·4
4580±2	581·1	(3)	0^-	<1		1·7
4559±2	601·9	1		6±1	2·5	
4503±2	658·2	1		4±1	6·7	
4449±2	711·7	1		—	0·6	
4416±2	744·6	1		5±1	11·0	
4390±2	771·3	1		5±1	11·2	
4366±2	795·4			3±1	0·6	
4126±2	1035·5	1		—		

[A] Data from Jurney *et al.* (1970). The thermal intensities in column 6 are normalized to 100 for the transitions shown here.
[B] Data from Kern *et al.* (1967).
[C] Relative intensity per 100 observed final state transitions.

Table 1 shows that transitions are observed to many of the low-lying states of ^{140}La. Where neighbouring final states were very close, the peaks were not fully resolved and individual intensities were unfolded from the data using gaussian line shapes and expected peak positions. In interpreting the various components, upper limits have been placed on the intensities of the weakest transitions.

The present data show that there is a strong tendency for transitions to occur to final states μ having $J_\mu^\pi = 2^-, 3^-, 4^-$ or 5^- (Table 2). This is expected since E1 transitions from s-wave resonances ($J_\lambda^\pi = 3^+$ and 4^+) to these states are possible. Transitions to 1^- and 6^- final states are allowed from p-wave capture (M1) and d-wave capture (E1). However, only d-wave resonances with $J_\lambda^\pi = 1^+$ and 6^+ can decay via E1 radiation to 0^- and 7^- final states. It is therefore possible to obtain an upper limit on the average d-wave capture cross section by calculating the relative intensities of transitions assuming that: (1) only dipole transitions are significant, (2) a $2J+1$ level density applies, (3) fluctuations in matrix elements are averaged out (in this case about 8% averaging accuracy), (4) an E_γ^3 energy dependence is applicable and (5) the ratio of radiative widths of E1 to M1 transitions is $\Gamma_{\lambda\mu}(\mathrm{E1})/\Gamma_{\lambda\mu}(\mathrm{M1}) \sim 5$. The calculated intensities (Table 2) are found to be comparable with the observed values when the cross sections are $\sigma_s \sim \sigma_p \lesssim 3\sigma_d$. Then the relative s-, p- and d-wave γ-ray intensities to the $l_n = 3$ states with $J_\mu^\pi = 3^-$ and 4^- are $1 : 0{\cdot}2 : \lesssim 0{\cdot}3$. Consequently, s-wave capture accounts for at least two-thirds of the γ-ray strength to the low-lying states, and the anomalous transitions cannot be attributed to d-wave capture. This result is supported by the thermal spectrum (Hughes *et al.* 1966; Jurney *et al.* 1970) which also exhibits strong transitions to the 3^- and 4^- states which can only result from s-wave capture.

Table 2. Comparison of observed and calculated intensities of transitions to final states in ^{140}La

J_f^π	No. of states	Observed intensity	Calculated intensity	J_f^π	No. of states	Observed intensity	Calculated intensity
0^-	1	<1	0·3	4^-	2	27	20·7
1^-	2	2·5	1·4	5^-	2	14	14·7
2^-	2	9·5	9·9	6^-	2	2·5	3·8
3^-	2	20	20·9	7^-	1	1	1·4

Discussion

In valence neutron capture, the incident neutron undergoes a change of state in the presence of a spectator core. Valence E1 neutron transitions to $l_n = 3$ states are forbidden by the triangle rule for the addition of angular momenta, because the change in orbital angular momentum exceeds unity. While d-wave valence capture is not forbidden, it cannot be the dominant mechanism in this case.

Additional support is therefore given to the argument (Allen *et al.* 1976) that a $2p$–$1h$ process is occurring. Possible neutron particle–hole pairs are $2f_{5/2}, 2d_{3/2}^{-1}$ and $3p_{1/2}, 3p_{3/2}$ particles coupled to $2d_{3/2}^{-1}, 3s_{1/2}^{-1}$ holes, e.g.

$$\pi(1g_{7/2}^{-1})\ \nu(2f_{7/2}, 3p_{1/2}, 2d_{3/2}^{-1}).$$

The energies of many of these pairs lie close to the γ-ray energies of the observed transitions (~5 MeV). The E1 particle–hole model is applicable only for s- and d-wave resonances, since positive-parity single-particle states are not found up to 1 MeV above the Fermi sea. Statistical spectra from p-wave resonances are therefore expected and the high energy γ-rays should be much weaker.

If the annihilation of the *p*–*h* pair leaves a neutron in the $f_{7/2}$ orbit coupled to an unperturbed core, final state correlations are expected between the (d, p) intensities and the corresponding γ-ray intensities. However, keV capture occurs through s-, p- and d-wave channels and thus γ-ray intensities need to be reduced by the calculated factors given in Table 2. Unfortunately, intensities to the 0^- and 7^- states are only upper limits and those to the 1^- and 6^- states have very large errors. These states cannot therefore be included in a correlation calculation, even though they comprise the strongest and weakest (d, p) intensities.

The above problems can be avoided by considering the relative intensities of transitions to pairs of like-spin states which have been split by the $|\pi(1g_{7/2})\rangle$ and $|\pi(2d_{5/2})\rangle$ quasi-proton states. Furthermore, the state vectors are linear combinations of these states coupled to the $f_{7/2}$ neutron, that is,

$$|JM\rangle_i = \alpha_i|\pi(1g_{7/2})\,\nu(2f_{7/2}):JM\rangle + \beta_i|\pi(2d_{5/2})\,\nu(2f_{7/2}):JM\rangle .$$

Since the ground state of ^{139}La is $|\pi(1g_{7/2})\rangle$, the (d, p) spectroscopic factor is proportional to α^2. Consequently, the relative intensities of (d, p) transitions to the states $|JM\rangle_1$ and $|JM\rangle_2$ reflect the single-particle nature of these states. If the *p–h* interaction in resonance capture leaves the core in an unperturbed state, then the (d, p) and (n, γ) intensities will be correlated. However, since the excitation energy of the $2d_{5/2}$ proton orbit in ^{139}La is only 166 keV, the core may well be left perturbed and in this case intensities will therefore be anticorrelated with the (d, p) strength.

Table 3. Ratios of transition intensities to 3^- and 2^- states in ^{140}La

E_x (keV)	Intensities to 3^- states (d, p)	thermal	keV	E_x (keV)	Intensities to 2^- states (d, p)	thermal	keV
0	9·3	3·4	8±1	30·0	9·9	<4·8	7±3
318·2	2·3	27·2	12±4	162·7	4·1	0·6	2·5±0·5
Ratio:	4·0	0·13	0·7±0·3	Ratio:	2·4	<8	2·8±1·2

Ratios are given in Table 3 for (d, p), thermal and averaged keV intensities to the 3^- and 2^- states. Ratios to other spin states are not available since the (d, p) intensities were not resolved. The ratios are seen to be comparable for the 2^- state, but appear anticorrelated for the 3^- state. These results cannot be explained on the statistical model because the ratios of intensities for both pairs of 2^- and 3^- spin states should be unity (i.e. independent of final state configuration). In average capture resonances, both unperturbed and excited target-state configurations may be present which favour transitions to similar components in the 2^- and 3^- final states respectively. Capture γ-ray spectra from single resonances are needed to confirm that transitions are either correlated or anticorrelated with the (d, p) strengths, but not both. The thermal data suggest that this is not the case.

It is of interest to search for initial state correlations between the reduced neutron widths and radiative widths of s-wave resonances. If the capture mechanism is dominated by an isolated common doorway, then large initial state correlations would be expected (Lane 1970). Recent high resolution measurements on ^{139}La (Musgrove *et al.* 1977) failed to find a correlation for 57 s-wave resonances. It appears therefore that a large number of overlapping doorway states exist in the threshold region in ^{139}La.

Conclusions

Neutron capture by ^{139}La in the 10–70 keV energy range shows transitions to many final states in the first MeV of excitation. The high energy structure is similar to that previously observed at the higher neutron energy of 210 keV and in thermal capture. Since little evidence is seen for d-wave capture, valence capture is eliminated as a dominant mechanism. The two-particle, one-hole capture mechanism remains a plausible qualitative explanation. However, spectra from individual s- and p-wave resonances are needed to confirm this hypothesis.

Acknowledgments

We wish to acknowledge discussions with A. R. de L. Musgrove. The authors thank R. Cawley and M. Scott for hardware and software developments in the PDP–15 computer and H. Broe, A. van Heugten and J. Fallon for technical assistance on the Van de Graaff accelerator.

References

Allen, B. J., Kenny, M. J., Barrett, R. F., and Bray, K. H. (1976). *Phys. Lett.* B **61**, 161.
Hughes, L. B., Kennett, T. J., and Prestwick, W. V. (1966). *Nucl. Phys.* **89**, 241.
Jurney, E. T., *et al.* (1970). *Phys. Rev.* C **1**, 2323.
Kenny, M. J., Allen, B. J., Boldeman, J. W., and Joye, A. M. R. (1976). *Nucl. Phys.* A **170**, 164.
Kern, J., Struble, G. L., and Sheline, R. K. (1967). *Phys. Rev.* **152**, 1331.
Lane, A. M. (1970). *Phys. Lett.* B **31**, 344.
Mughabghab, S. F., and Garber, D. J. (1973). Brookhaven National Lab. Rep. No. BNL–325.
Musgrove, A. R. de L., Allen, B. J., and Macklin, R. L. (1970). *Aust. J. Phys.* **30**, 599.
Spits, A. M. J., Op der Kamp, A. M. F., and Grüppelaar, H. (1971). *Nucl. Phys.* A **145**, 469.

Manuscript received 15 April 1977